Proceedings of the 17th International Conference on Automation & Computing, University of Huddersfield, Huddersfield, UK, 10 September 2011

The Effect of Depth of Cut on the Molecular Dynamics (MD) Simulation of Multi-Pass Nanometric Machining

A.O. Oluwajobi[1] and X. Chen[2]
Centre for Precision Technologies
University of Huddersfield
Queensgate, Huddersfield HD1 3DH, UK
[1]j.o.oluwajobi@hud.ac.uk, [2]x.chen@hud.ac.uk

Abstract— **The effect of depth of cut on multi-pass nanometric machining of copper workpiece with diamond tool was studied using the Molecular Dynamics (MD) simulation. The copper-copper interactions were modelled by the EAM potential and the copper-diamond interactions were modelled by the Morse potential. The diamond tool was modelled as a deformable body and the Tersoff potential was applied for the carbon-carbon interactions. It was observed that the average tangential and normal components of the cutting forces increase with increase in depth of cut and they reduced in consecutive cutting passes for each depth of cut. Also, the ratio of the tangential to normal force components decreases as the depth of cut increases, but remains fairly constant after 1.5nm depth of cut. The ratio of the cutting force to area decreases with increase in the depth of cut and remains constant after 2.5nm depth of cut.**

Keywords- Multi-Pass; Depth of Cut, Molecular Dynamics; Nanometric Machining, Cutting Forces

I. INTRODUCTION

.

Current material removal technological requirements in the aerospace, automobile, medical and energy industries are at the nanoscale, with stringent form and surface finish accuracy. At this length scale, machining phenomena take place in a small limited region of tool – workpiece interface, which often contains a few atoms or layers of atoms. At present, it is very difficult to observe the diverse microscopic physical phenomena occurring through experiments at the nanoscale [1]. The interface at this nanometre level may not be considered as a continuous media or homogeneous as assumed by continuum mechanics, so the analysis should be based on discrete atoms, whose interactions are governed by appropriate interatomic potentials. The use of Molecular Dynamics (MD) simulation has proved to be an effective tool for the investigation of machining processes at the nanometre scale. The method gives higher resolution of the cutting process than what is possible by continuum mechanics on that length scale [2].

The MD method was initiated in the late 1950s at Lawrence Radiation Laboratory in the US by Alder and Wainwright in the study of statistical mechanics [3]. Since then, the use of the simulation method has extended from Physics to Materials Science and now to Mechanical Engineering. Rentsch and Inasaki [4] modelled a copper workpiece and a diamond tool using the Lennard-Jones potential for the copper atom interactions. They observed a build-up phenomenon after 25000 time steps, while keeping the tool rigid. Komanduri et al [5] used copper workpiece and an infinitely hard tungsten tool for their simulation. They used Morse potentials and a cutting speed of 500m/s.

Many existing MD simulation studies on nanometric cutting have been limited to single pass or simple line-type groove. As an extension of the single pass studies, Zhang et al [6] modelled folder- line grooves for AFM-based nanometric cutting process of copper workpiece with diamond tool. They used the EAM potential for the copper-copper interactions and the Morse potential for the copper-diamond interactions. They treated the diamond tool as rigid and concluded that the normal, lateral and the resultant forces were almost symmetric with respect to the critical folder angle of 45°. Shi et al [7] investigated the multi-groove simulation of single-point tuning of copper workpiece with diamond tool. They used two diamond tools, offset by a fixed distance to simulate a two-groove cutting and modelled the copper-copper and the copper-diamond interactions by using the Morse potential. They also treated the tool as a rigid body and observed that the tool forces increase with increase in feed rate and depth of cut. In practice, most machining processes involve the use of multiple passes to create new surface patterns and the diamond tool is deformable and subjected to wear. This study clearly shows the consecutive passes of cut, which is novel in multi-pass nanometric machining MD simulations. Also, the effect of the variation of depth of cut on the simulation of multi-pass cutting was investigated to model the surface creation in single point diamond turning.

II. THE MD METHODOLOGY

The nanometric cutting model consists of a monocrystalline copper workpiece and a diamond tool.

The model configuration has a total of 54232 atoms as shown in Fig. 1. The workpiece is made up of 43240 copper atoms, with the face-centred cubic (FCC) lattice. It includes 3 kinds of atoms namely; boundary atoms, Newtonian atoms and thermostat atoms (See Fig. 1). The cutting tool has 10992 carbon atoms with diamond lattice structure. Fig. 2a shows a diagram of the machined grooves with passes 1 - 3 and Fig. 2b shows the tool tip dimensions, with the upper part as variable, which depends on the depth of cut considered.

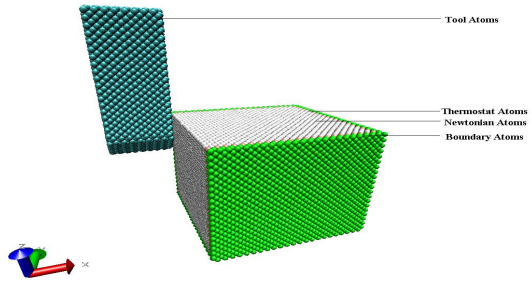

Figure 1: The MD Simulation Model

The end of the cutting tool is trapezoidal shaped (fairly pointed, with a blunt end). For the workpiece, the boundary atoms are kept fixed to reduce edge effects.

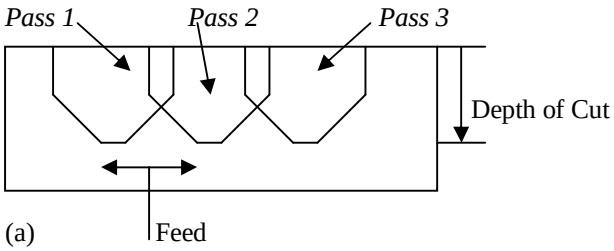

(a)

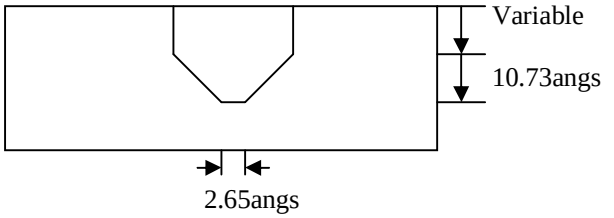

(b)

Figure 2a: Cross Section of the Machined Grooves with Passes 1-3 (direction of cut is perpendicular to the paper face) 2b: Tool Tip Dimensions

The Newtonian atoms obey the Newton's equation of motion. The thermostat atoms conduct the heat generated during the cutting process out of the cutting region. This is achieved by the velocity scaling of the thermostat atoms, (with the conversion between the kinetic energy (KE) and temperature via Eq. 1 [8, 9]);

$$\sum_i \frac{1}{2} m_i v_i^2 = \frac{3}{2} N k_B T_i \qquad (1)$$

Where m_i is the mass of the ith atom, v_i is the resultant velocity of the ith atom, N is the number of the thermostat atoms, T_i is the temperature of the ith atom and k_B is the Boltzmann constant (1.3806504 x10^{-23} JK^{-1})

Whenever the temperature of the thermostat atoms exceeds the preset bulk temperature of 293K, their velocities are scaled by using Eq. 2 [10, 11];

$$v_{i,new} = v_i \sqrt{\frac{T_{desired}}{T_{current}}} \qquad (2)$$

Where $v_{i,new}$ is the newly scaled velocity of atom i, v_i is the velocity of atom i, $T_{current}$ is the current temperature that is calculated from the KE and the $T_{desired}$ is the desired temperature.

The simulation conditions applied in this study are the following, viz; bulk temperature is 293K, the cutting direction is along the x-axis, the cutting speed is 150m/s, the feed is 1.5nm, the time step is 0.3fs and the simulation run is 150000 steps. The depths of cut used are 0.5nm, 1.0nm, 1.5nm, 2nm, 2.5nm and 3 nm. The LAMMPS parallel MD software [12] was used for the simulations, on the University of Huddersfield's High Performance Computing (HPC) grid, with a total of 144 processing cores (36 nodes) and a RAM of 8 GB (800Mhz) per node. The MD software utilized 2 nodes and 4 processors for each simulation. The VMD software [13] was used for the visualization of the results.

III. THE MODELLING PARAMETERS FOR THE SIMULATION

It has been previously established that the EAM potential is very suitable for the Cu-Cu interactions [14], [15] and for the Cu-C interactions; the Morse potential is a good choice [16].

A. Embedded-Atom Method Potential (EAM) (Eq. 3) [17] (For the Cu-Cu interactions)

$$E_{tot} = \sum_i G_i(\rho_{h,i}) + \frac{1}{2}\sum_{i,j} V_{ij}(r_{ij}) \qquad (3)$$

Where E_{tot} is the total embedding energy, $\rho_{h,i}$ is the total electron density at atom i due to the rest of the atoms in the system, G_i is the embedding energy for placing an atom into the electron density, $V_{i,j}$ is the short range pair interaction representing the core-core repulsion, r_{ij} is the separation of atoms i and j.

B. Morse Potential (Eq. 4) [18]
(For the Cu-C interactions)

$$V_{ij} = D\{\exp[-2\alpha(r_{ij} - r_e)] - 2\exp[-\alpha(r_{ij} - r_e]\} \quad (4)$$

Where V_{ij} is the pair potential, r_{ij} and r_e are instantaneous and equilibrium distances between atoms *i* and *j* respectively, α and D are constants determined on the basis of the physical properties of the material.

The parameters used in the simulations are below, [19];

$D = 0.087eV,\ \alpha = 0.17(nm)^{-1},\ r_e = 0.22nm$

The cut-off distance chosen was 6.4 Angstroms (that is, the interactions between atoms separated by more than this distance are neglected).

B. Tersoff Potential (Eq. 5) [20]
(For the C-C interactions)

$$E = \sum_i E_i = \frac{1}{2}\sum_i \sum_{i \neq j} V_{ij} \quad (5)$$

and,

$$V_{ij} = f_C(r_{ij})[a_{ij} f_R(r_{ij}) + b_{ij} f_A(r_{ij})]$$

where

$$f_R(r) = A\exp(-\lambda_1 r),$$

$$f_A(r) = -B\exp(-\lambda_2 r),$$

$$f_C(r) = \begin{cases} 1, & r < R - D \\ \frac{1}{2} - \frac{1}{2}\sin\left[\frac{\pi}{2}(r - R)/D\right], & R - D < r < R + D \\ 0, & r > R + D \end{cases},$$

$$b_{ij} = (1 + \beta^n \zeta_{ij}^n)^{-1/2n},$$

$$\zeta_{ij} = \sum_{k(\neq i,j)} f_C(r_{ik}) g(\theta_{ijk}) \exp\left[\lambda_3^3 (r_{ij} - r_{ik})^3\right],$$

$$g(\theta) = 1 + \frac{p^2}{q^2} - \frac{p^2}{\left[q^2 + (h - \cos\theta)^2\right]},$$

$$a_{ij} = (1 + \alpha^n \eta_{ij}^n)^{-1/2n},$$

$$\eta_{ij} = \sum_{k(\neq i,j)} f_C(r_{ik}) \exp\left[\lambda_3^3 (r_{ij} - r_{ik})^3\right]$$

Where E, E_i are the energies of interacting atoms, V_{ij} is the pair potential, R and D are cut-off parameters; $A, B, \lambda_1, \lambda_2, \lambda_3, \alpha, \beta, n, p, q, h$ are fitting parameters of the Tersoff potential.

The simulation parameters used for carbon, are given as [20, 21, 22];

A(eV) = 1.3936×10^3; B(eV) = 3.467×10^2;

$\lambda_1(nm^{-1})$ = 34.879; $\lambda_2(nm^{-1})$ = 22.119; α = 0.0;

β = 1.5724×10^{-7}; n = 7.2751×10^{-1}; p = 3.8049×10^4;

q = 4.384; h = -5.7058×10^{-1};

$\lambda_3(nm^{-1})$ = 22.119; R (nm) = 0.18; D(nm) = 0.02.

(F_x, F_y, F_z : are the tangential, lateral and normal components of the cutting forces respectively (eV/Angs = 1.602×10^{-9}N)).

It should be noted that, generally, the interatomic potential parameters used for MD simulations are verified by ascertaining good agreement between their predicted values of the material properties and experimental data.

IV. SIMULATION RESULTS

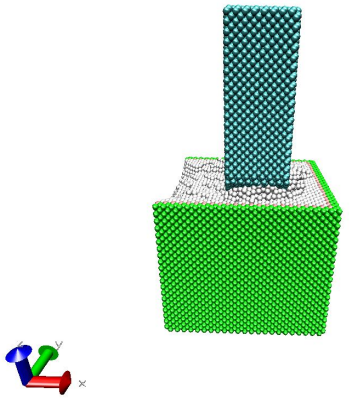

Figure 3: Simulation of Depth of Cut 0.5nm – Pass 3

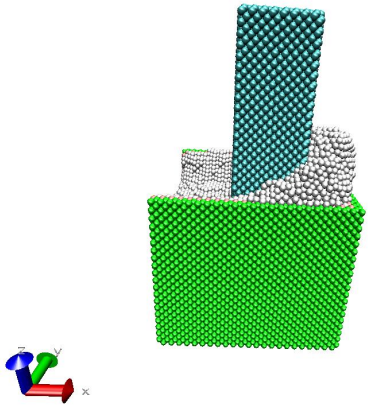

Figure 4: Simulation of Depth of Cut 1.5nm – Pass 3

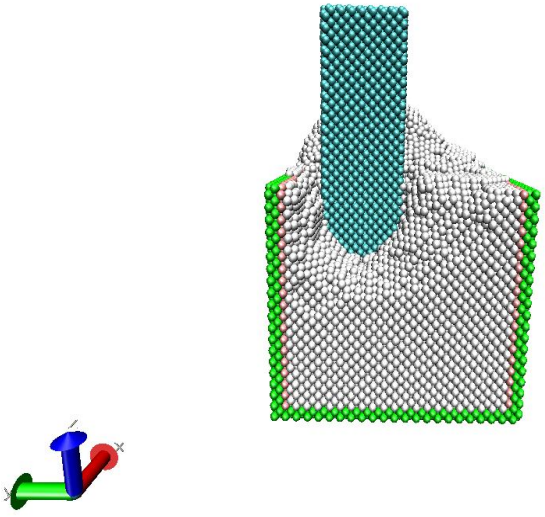

Figure 5: Simulation of Depth of Cut 3nm – Pass 1

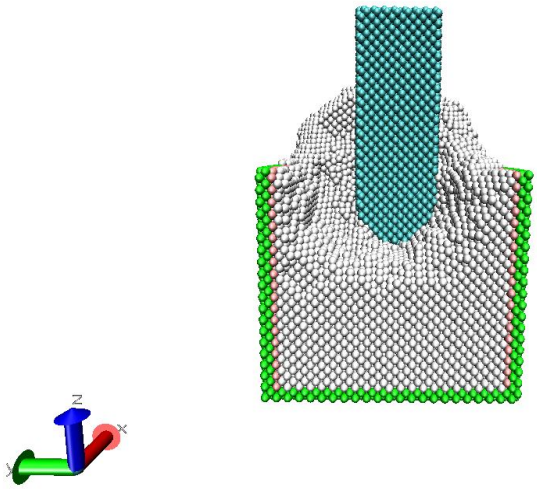

Figure 6: Simulation of Depth of Cut 3nm – Pass 2

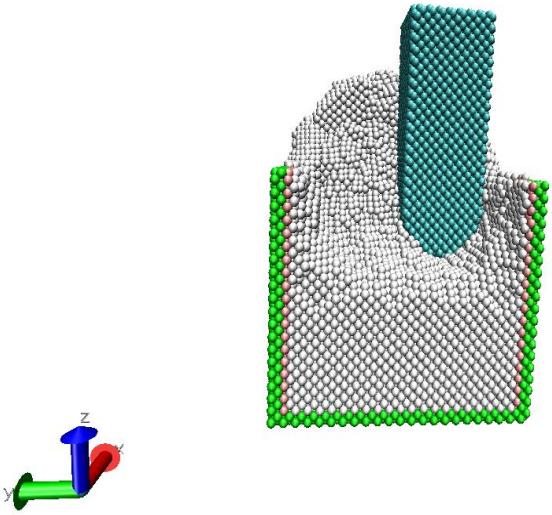

Figure 7: Simulation of Depth of Cut 3nm – Pass 3

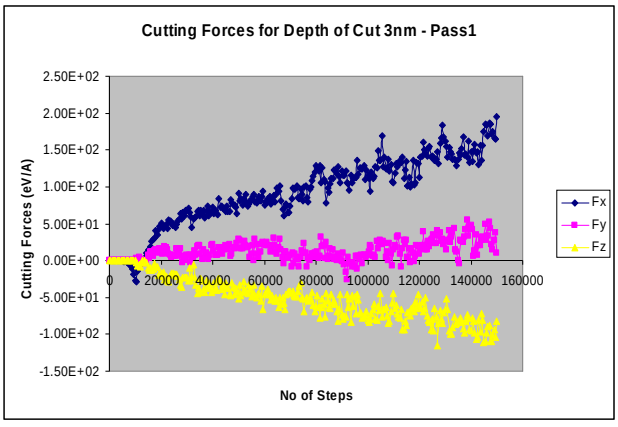

Figure 8: Cutting Forces for Depth of Cut 3nm – Pass 1

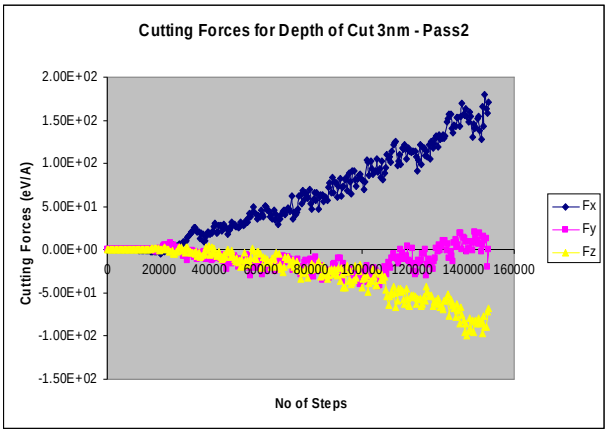

Figure 9: Cutting Forces for Depth of Cut 3nm – Pass 2

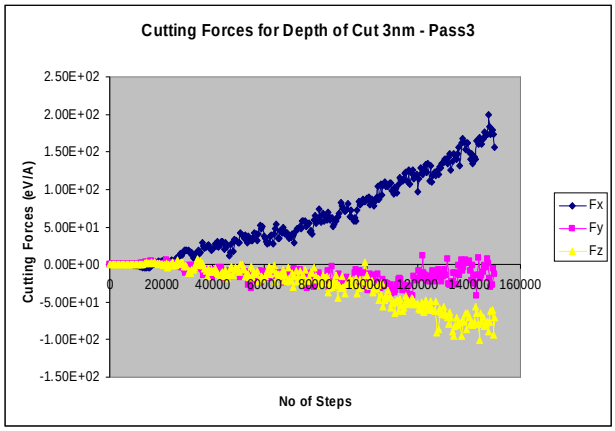

Figure 10: Cutting Forces for Depth of Cut 3nm – Pass 3

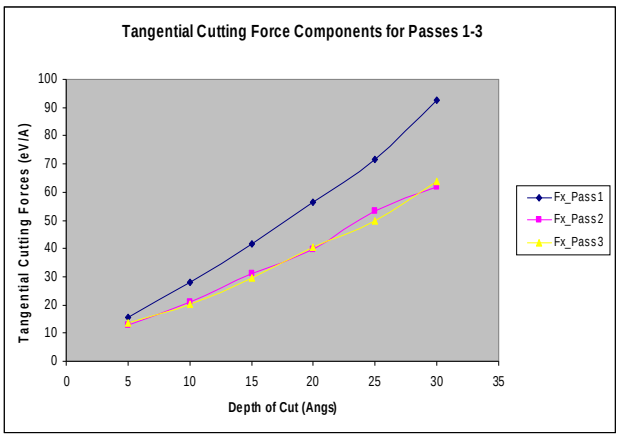

Figure 11: Variation of F_x in Passes 1-3 with Depth of Cut

V. RESULTS AND DISCUSSION

Figs. 3 and 4 show the simulations after the third pass for the depth of cut of 0.5nm and 1.5nm respectively. From the figures, it can be observed that the amount of atoms removed increases as the depth of cut increases, which is logical, because as the depth increases, there is more volume of material atoms to be removed.

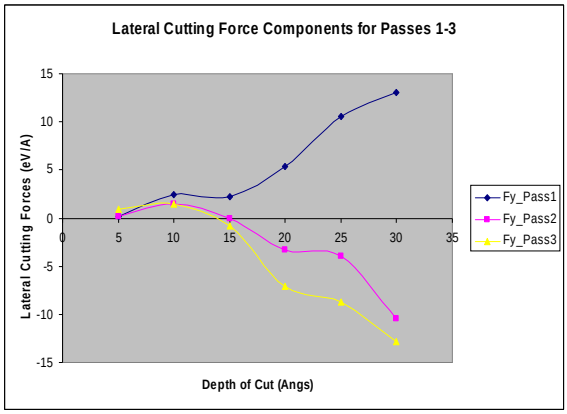

Figure 12: Variation of F_y in Passes 1-3 with Depth of Cut

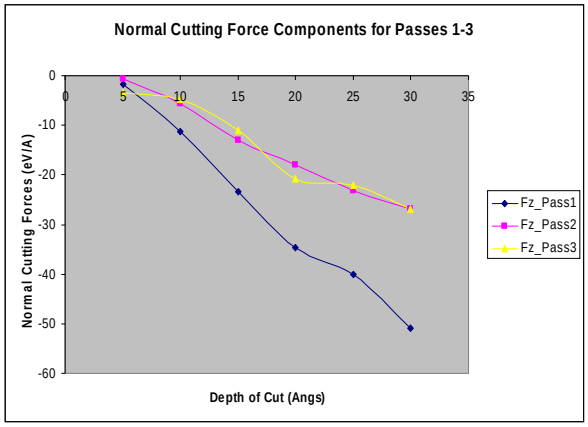

Figure 13: Variation of F_z in Passes 1-3 with Depth of Cut

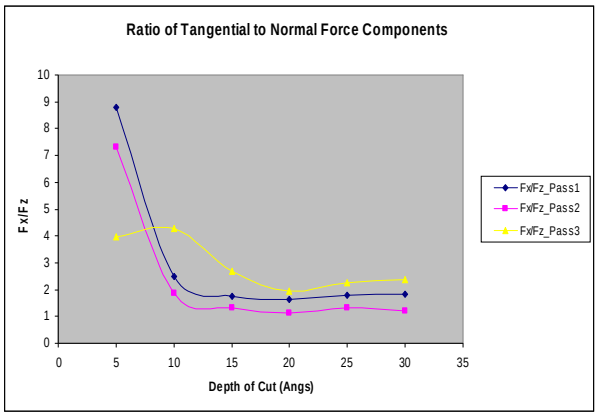

Figure 14: Variation of F_x/F_z in Passes 1-3 with Depth of Cut

Figs. 5-7 show the simulation of the three consecutive passes for the depth of cut of 3nm and Figs. 8-10 show the associated cutting forces respectively. The average tangential and the normal cutting force components decrease with the consecutive passes. Figs. 11-13 show the variation of the cutting force components, (F_x, F_y and F_z) with depth of cut, for passes 1-3. It can be seen that for the different passes, both F_x and F_z increase in magnitude with increase in the depth of cut. The average values of F_x and F_z are larger in pass 1 than in passes 2 and 3. Also, the values for passes 2 and 3 are quite close. This is because the cutting cross sectional area for passes 2 and 3 are similar. The variation of F_y is considerably smaller than both F_x and F_z, and it should be zero theoretically. The small variation is due to the atomic vibration during the cutting process. For pass 1, F_y is positive and becomes negative for passes 2 and 3 after the depth of cut of 1.5nm.

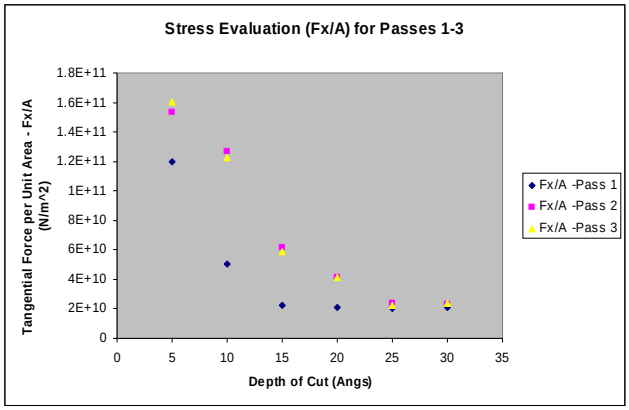

Figure 15: Stress Variation with Depth of Cut for Passes 1-3

The change from positive to negative is because for passes 2 and 3, the structure of the workpiece to be cut becomes asymmetrical and skewed to the right. Fig. 14 shows the ratio F_x/F_z, which is a measure of friction for the different passes. It can be seen that this ratio is fairly constant after the depth of cut of 1.5nm, which might be due to the tool geometry. Fig. 15 shows the stress variation with depth of cut for the three passes. It can be observed that as the depth of cut increases, the stress values decrease and it is higher for passes 2 and 3. The stress values are in the range from 160GPa to 20GPa. The values remain constant at around 20 GPa for all passes for higher depth of cut – from 2.5nm. This is due to the tool geometry, which becomes similar for higher depths of cut. The highest stress values are for depth of cut of 0.5nm during passes 2 and 3. It shows that the cutting resistance of the copper material is highest at very small depth cuts.

VI. CONCLUSION

The simulation of multi-pass nanometric machining has been conducted by using the MD method, and the effect of varying the depth of cut has been investigated. Some important results are hereby outlined. The magnitude of the tangential and the normal components of the cutting forces increase with the increase in the depth of cut. The ratios of the tangential to normal force components decrease as the depth of cut increases, but remain fairly constant for each of the passes after 1.5nm depth of cut, with values in the range of 1.1-2.3. Stress values decrease with increase in the depth of cut and remain constant for high depth of cut.

REFERENCES

[1] Rentsch, R., "Nanoscale cutting", in Davim, J.P. and Jackson, M.J. (Eds.): Nano and Micromachining, Wiley-ISTE, 2008, pp. 1–24

[2] Komanduri R. and L.M. Raff, "A Review on the Molecular Dynamics Simulation of Machining at the Atomic Scale", Proceedings of the Institution of Mechanical Engineers, Part B: Journal of Engineering Manufacture, Vol. 215, No. 12, 2001, pp. 1639-1672

[3] Alder B.J.and T.E. Wainwright, "Studies in Molecular Dynamics. I. General Method", Journal of Chemical Physics, Vol 31, 1959, pp. 459-466

[4] Rentsch R. and I. Inasaki, "Molecular Dynamics Simulation for Abrasive Processes", Annals of the CIRP Vol. 43, No 1, 1994, pp. 327-330

[5] Komanduri R., N. Chandrasekaran and L.M. Raff, "Some Aspects of Machining with Negative-Rake Tools Simulating Grinding: A Molecular Dynamics Simulation Approach", Philosophical Magazine Part B, Vol. 79, No 7, 1999, pp. 955-968

[6] Zhang J.T. , T. Sun, Y. Yan, Y. Liang and S. Dong, "Molecular Dynamics Study of Groove Fabrication Process using AFM-Based Nanometric Cutting Technique", Applied Physics A (Materials Science and Processing), Vol. 94, 2009, pp. 593-600

[7] Shi J., Y. Shi and C.R. Liu, "Evaluation of a Three-Dimensional Single-Point Turning at Atomistic Level by a Molecular Dynamics Simulation", International Journal of Advanced Manufacturing Technology, Vol. 45, Nos 1-4, 2011, pp. 161-171

[8] Cai M., X. Li and M. Rahman, "Molecular Dynamics Modelling and Simulation of Nanoscale Ductile Cutting of Silicon", International Journal of Computer Applications in Technology, Vol. 28, No. 1, 2007, pp 2-8

[9] Guo Y., Y. Liang, M. Chen, Q. Bai and L. Lu, "Molecular Dynamics Simulations of Thermal Effects in Nanometric Cutting Process", Science China Technological Sciences, Vol. 53, No. 3, 2010, pp. 870-874

[10] Cheong W.C.D., L. Zhang and H. Tanaka, "Some Essentials of Simulating Nano-Surface Processes using the Molecular Dynamics Method ", Key Engineering Materials, Vol. 196, 2001, pp. 31-42

[11] Lin Z.-C. Z.-D. Chen and J.-C. Huang, "Establishment of a Cutting Force Model and Study of the Stress-Strain Distribution in Nano-scale Copper Material Orthogonal Cutting", International Journal of Advanced Manufacturing Technology, Vol. 33, No. 5-6 2007, pp. 425-435

[12] Plimpton S. J., "Fast Parallel Algorithms for Short-Range Molecular Dynamics", J Comp Phys, Vol. 117, 1995, pp. 1-19 and www.lammps.sandia.gov

[13] Visual Molecular Dynamics (VMD), http://www.ks.uiuc.edu/Research/vmd/ (Accessed in 2010)

[14] Oluwajobi A.O. and X. Chen, "The Effect of Interatomic Potentials on Nanometric Abrasive Machining", Proceedings of the 16th International Conference on Automation and Computing, 2010, pp. 130-135

[15] Oluwajobi A.O. and X. Chen, "The Fundamentals of Modelling Abrasive Machining Using Molecular Dynamics", International Journal of Abrasive Technology, Vol. 3, No. 4. 2010, pp. 354-381

[16] Pei Q.X., C. Lu, F.Z. Fang and H. Wu, 'Nanometric Cutting of Copper: A Molecular Dynamics Study', Comp.Mat. Sci., Vol. 37, 2006, pp. 434-441

[17] Foiles S.M., "Application of the Embedded Atom Method to Liquid Transition Metals", Physical Review B, Vol. 32 No 6, 1985, pp. 3409-3415

[18] Morse P.M., "Diatomic Molecules according to Wave Mechanics II Vibrational Levels", Physical Review Vol. 34, 1929, pp. 57-64

[19] Hwang H.J., O-K Kwon and J. W. Kang, "Copper Nanocluster Diffusion in Carbon Nanotube", Solid St. Comm. 129, 2004, pp. 687-690

[20] Tersoff J., "Empirical Interatomic Potential for Silicon with Improved Elastic Properties", Physical Review B, Vol. 38 No 14, 1988, pp. 9902-9905

[21] Raffi-Tabar H. and G.A. Mansoori, "Interatomic Potential Models for Nanostructures", in Encyclopedia of Nanoscience and Nanotechnology, ed. H.S. Nalwa, American Scientific Publishers, Vol X, 2003, pp. 1-17

[22] Saito Y., N. Sasaki, H. Moriya, A. Kagatsume and S. Noro, "Parameter Optimization of Tersoff Interatomic Potentials Using Genetic Algorithms", JSME International Series A, Vol. 44, No. 2, 2001 pp. 207-213